Applied Catalysis B: Environmental 87 (2009) 162–170

Contents lists available at ScienceDirect

Applied Catalysis B: Environmental

journal homepage: www.elsevier.com/locate/apcatb

The influence of ultrasound on the RuI_3-catalyzed oxidation of phenol: Catalyst study and experimental design

Ekaterina V. Rokhina [a,*], Manu Lahtinen [b], Mathias C.M. Nolte [c], Jurate Virkutyte [a]

[a] Department of Environmental Science, University of Kuopio (KY), FI-70211 KY, Finland
[b] Department of Chemistry, University of Jyväskylä (JY), FI-40014 JY, Finland
[c] Institute of Environmental Technology and Energy Economics, Technische Universität Hamburg-Harburg, Eißendorfer Straße 40, 21073 Hamburg, Germany

ARTICLE INFO

Article history:
Received 20 June 2008
Received in revised form 4 September 2008
Accepted 10 September 2008
Available online 19 September 2008

Keywords:
Ultrasound
Phenol
Ruthenium iodide
Oxidation
Experimental design

ABSTRACT

The influence of ultrasound at 24 kHz on the heterogeneous aqueous oxidation of phenol over RuI_3 with hydrogen peroxide (H_2O_2) was studied isothermally at 298 K. Effect of ultrasound irradiation on catalytic properties and performance of RuI_3 has been studied in details by means of scanning electron microscopy (SEM), X-ray powder diffraction (XRD), dispersion analyzer and a surface analyzer. Turn over frequency of the catalyst was also calculated. In this work, experimental design methodology was applied to optimize the degradation of phenol in aqueous solution, while minimizing an excessive consumption of chemical reagents. The independent variables considered were the catalyst load and oxidant concentration. The multivariate experimental design allowed the development of empiric non-linear quadratic models for total organic carbon (TOC) removal after 120 and 240 min of the reaction, and the time needed for total hydrogen peroxide consumption, which were adequate to predict responses in all of the range of experimental conditions used. Ruthenium leaching was not detected from samples studied at different stages of the reaction, indicating stability of the chosen catalyst. A reaction scheme involving radical species ($^{\bullet}OH$, $^{\bullet}HO_2$) was proposed to explain phenol conversion. Ultrasound-assisted catalytic oxidation demonstrated nearly two-fold increase in phenol conversion (up to 70%), contrary to 31% obtained during silent process. High catalytic activity of RuI_3 associated with isothermal reaction conditions at circum neutral pH was capable to extend the applicability of such catalyst in ultrasound-assisted oxidation processes.

1. Introduction

Last decade's research on chemical effects of ultrasound (US) has been applied to heterogeneous catalysis and chemical oxidation [1–6]. The effects of ultrasonic irradiation on heterogeneous catalysis can be divided into three groups: (i) those that alter the formation of heterogeneous catalysts, (ii) those that perturb the properties of previously synthesized catalysts, and (iii) those that affect catalyst reactivity during catalysis. In practice, these three classes of effects are often deeply intertwined in reported experimental results [1]. The use of ultrasound for oxidation purposes has been reported as "hot spot theory". The theory accounts radicals production as crucial reactive species in advanced oxidation processes (AOPs) as a result of water dissociation upon thermal reaction during the final step of the collapse of cavitation bubbles that are formed due to acoustic cavitation in a liquid, irradiated with ultrasound [1–3]. The formation and recombination of radicals gives rise to the following reactions, which occur almost simultaneously:

$$H_2O \xrightarrow{)))} {}^{\bullet}OH + {}^{\bullet}H \quad (1)$$

$$^{\bullet}OH + {}^{\bullet}H \rightarrow H_2O \quad (2)$$

$$2\,{}^{\bullet}OH \rightarrow H_2O + \tfrac{1}{2}O_2 \quad (3)$$

$$2\,{}^{\bullet}OH \rightarrow H_2O_2 \quad (4)$$

$$2\,{}^{\bullet}H \rightarrow H_2 \quad (5)$$

In the presence of solid metal particles and H_2O_2, all formed species are involved in so-called Weiss mechanism for metal-catalyzed decomposition of H_2O_2, generally accepted

* Corresponding author. Tel.: +358 440176196.
E-mail address: katja.rokhina@uku.fi (E.V. Rokhina).

0926-3373/$ – see front matter © 2008 Elsevier B.V. All rights reserved.
doi:10.1016/j.apcatb.2008.09.006

for AOPs [3]:

$$Me + H_2O_2 \rightarrow Me^+ + OH^- + {}^{\bullet}OH \quad (6)$$

$$Me^+ + {}^{\bullet}O_2{}^- \rightarrow Me + O_2 \quad (7)$$

$$Me + {}^{\bullet}HO_2 \rightarrow Me^+ + HO_2{}^- \quad (8)$$

$$Me^+ + HO_2{}^- \rightarrow Me + {}^{\bullet}HO_2 \quad (9)$$

Nowadays, sonochemically assisted heterogeneous catalytic oxidation of phenol is increasing in popularity [4–10]. Catalysts employed in most previous studies have been primarily Fenton and Fenton-like reagents [4–6], copper oxide [7], enzymes [8], TiO_2 [9], and CuO·ZnO supported on alumina catalyst [10]. However, several disadvantages for reported systems have been observed, such as the necessity to adjust pH for Fenton-like processes and usually low lifetime of the catalyst [5,8]. The oxidation of phenols generally lacks selectivity because of coupling reactions caused by phenoxyl radicals, and selective oxidation of phenols is limited to phenols bearing bulky substituent at the 2- and 6-positions [11].

Therefore to overcome the present drawbacks, the current study is aimed at the oxidation of aqueous phenol over RuI_3 powder catalyst without the adjustment of initial pH and high potential reusability and significantly higher lifetime of the catalyst. Ru(III) catalysis involves several complexes, forming different active species and shows capability to decompose hydrogen peroxide with further generation of hydroxyl radicals [12].

In the present work two types of studies are discussed. First, a detailed catalyst study is carried out to describe the influence of ultrasound on catalyst characteristics and performance. The purpose of this investigation is to address issues pertaining to variable catalytic activity after ultrasound irradiation, necessary to achieve desirable conversion rate of phenol. Second, oxidation of phenol is represented as a chain reaction employing approximate scheme of the process with determination of reactive species and the rate-limiting step of the reaction. Furthermore, differences in the reaction rates in silent versus ultrasound-assisted catalytic oxidation are determined and explained. Finally, factorial experimental design has been applied to study the influence of various operational parameters in the reaction as a novel approach to optimize the process parameters.

2. Experimental

2.1. Materials

Phenol, RuI_3, H_2O_2 (30%), methanol, methyl tert-butyl ether (MTBE) and other chemicals were of laboratory reagent grade and used without further purification. All chemicals were purchased from Sigma–Aldrich and Merck & Co., Inc. All the solutions were prepared using high purity deionized water (>17.7 MΩ).

2.2. Catalyst characterization

The specific surface area, pore volume, and the pore size distribution of the samples were measured and calculated according to the BET method on a Quantachrome Autosorb 1 analyzer (Quantachorome instruments, UK) with liquid nitrogen at −196 °C. The BJH method was used to determine the pore size distribution. Prior to measurements, all samples were degassed at 623 K for 4 h. Particle size distribution was assessed by means of dispersion analyzer LUMIsizer (L.U.M. GmbH, Germany). The filtrate was subjected to ICP–OES (iCAP 6000, UK) analysis to assess the potential leaching of Ru(III) ions to the solution, as a result of RuI_3 dissolution with detection limit for Ru ions of 0.003151 ppm. The surface morphology of the catalyst samples was observed by scanning electron microscopy (SEM) using a Leo Gemini 1530 apparatus (USA), EDX at 20 kV for the imaging in in-lens mode at 10 kV. The X-ray powder diffraction (XRD) data was observed with PANalytical X'Pert PRO diffractometer in Bragg–Brentano geometry using Johansson monochromator (α_1 setup) to produce pure Cu $K\alpha_1$ radiation (1.5406 Å; 40 kV, 30 mA) and step-scan technique in 2θ range of 4–100°.

Turn over frequency of the catalysts TOF (h^{-1}) was calculated as a number of moles of phenol converted per mole of catalyst in 1 h.

The catalyst particles agglomeration kinetics has been calculated as traditional interpretation of the power law:

$$-\frac{dS}{dt} = k_s S_{cat} \quad (10)$$

where S_{cat} is a surface area of the catalyst ($m^2\,g^{-1}$).

2.3. Catalytic oxidation of phenol and analyses

The catalytic oxidation of phenol (100 ppm) over RuI_3 as a catalyst was studied in a 100 mL glass reactor equipped with magnetic stirrer and a temperature controller. The reaction mixture was stirred at a speed of 800 rpm for 1–6 h to provide a complete mixing for uniform distribution and full suspension of catalysts particles. No mechanical stirring of the solution was performed during sonication due to the disturbance caused by cavitation bubble oscillation and collapse, providing itself an extremely efficient mixing. Ultrasound irradiation of the solution was carried out with an ultrasonic transducer UP 400H (Hielscher, Germany) with horn-type sonicator, capable of operating either continuously or in a pulse mode at a fixed frequency of 24 kHz and a maximum electric power output of 400 W. The actual ultrasonic power dissipated in the process vessel was determined by adopting the procedure reported by Hagenson and Doraiswamy [13]. Immersion circulator unit (Mo 1112A, VWR, UK) was used to maintain a constant ambient temperature throughout experiments. For experiments, unless specified otherwise, untreated catalyst (0.5–2 $g\,L^{-1}$) was introduced as a suspension to the reaction medium with following H_2O_2 (30%), (200–1200 ppm) addition. Samples were taken at regular intervals for the subsequent analysis and filtered through syringe filter (0.45 μm hydrophilic Millipore filter) to separate the catalyst particles from the solution. The pH of filtrate was then determined by a pH meter (3401 WTW, Germany). The degradation of phenol was monitored by UV–Vis spectroscopy at λ = 268.4 nm (PerkinElmer UV–Vis Spectrometer Lambda 45, US) [14]. The progress of the catalytic decomposition was monitored by measuring total organic carbon (TOC analyzer, TOC-5000, Shimadzu Seisakusho Co., Japan) at various time intervals. H_2O_2 was measured spectrophotometrically using dual-wavelength method by UV–Vis spectrophotometer [15]. The potential reusability of the catalyst was evaluated by reclaiming the catalyst after reaction in the batch mode, washing and drying in air at 378 K and using it for further phenol degradation under similar experimental conditions. To monitor catalyst deactivation in all cases, the experimental tests were performed in five cycles using a model solution. The first cycle was carried out in duplicate to provide enough amount of catalyst to continue the following tests. In order to ascertain the leading part of radicals for current process efficiency, the qualitative detection of free radicals has been performed by means of a strong radical scavenger (methanol and methyl tert-butyl ether (MTBE) in different concentrations of 100, 500 and 1000 ppm), as it has been described elsewhere [16].

2.4. Experimental design

The object of the methodology of experimental research is to search for an optimal strategy which allows obtaining the largest number of good quality information concerning a studied phenomenon, while carrying a limited number of experiments [17]. These are informationally optimal mathematical schemes in which all important factors are changed simultaneously, thereby facilitating the identification of process relations as well as the location of the real process optimum.

2.4.1. Fractional factorial design

Fractional factorial design 3^2 was chosen to evaluate the factors that significantly influence degradation of phenol in terms of TOC decrease, since TOC reduction is a direct measure of the extent of mineralization, which is highly dependent on the availability of oxidizing agents. The model function is written as follows:

$$Y = b_0 + \sum b_i x_i + \sum b_{ij} x_i x_j + \cdots + b_{12\ldots k} x_1 \ldots x_k \quad (11)$$

For the present work, the influence of two factors was evaluated. A factor is an assigned variable and the levels of the factor are the values assigned to that factor. Each experiment represents a particular point of the experimental domain, and provides a measurement with one or several responses of the phenomenon in this point. The independent variables selected were the main reaction parameters: catalyst and oxidant concentrations. The influence of the most significant effects such as RuI_3 and H_2O_2 concentrations of 0.5, 1.0 and 1.5 g L^{-1} and 200, 800 and 1200 ppm respectively, were assessed, and time of full hydrogen peroxide consumption was tested under similar conditions. The real values of independent variables were coded as −1, 0 and 1 for low, medium and high levels, respectively. The effect of the parameters was determined by alteration of TOC at 120 and 240 min. The influence of H_2O_2 decomposition time was assessed by means of the time required to achieve total consumption of hydrogen peroxide. The values of experimental results and results obtained from the model are presented in Table 1. Coded variables x_1 and x_2 corresponded to RuI_3 and H_2O_2 initial concentrations, respectively. The response variables of TOC conversion at 120 and 240 min (Y_1 and Y_2) and the time required to achieve total consumption of hydrogen peroxide (T) were selected for the study of activity of the system in phenol conversion with ultrasound-assisted catalytic oxidation.

In a general case, a design point number (number of trials different stages of research subject) depends on factor level number and therefore may be calculated according to:

$$N = p^k \quad (12)$$

where N is a number of design points trials; p is a number of factor levels and k is a number of factors. All experiments were performed in randomized order to minimize the effect of uncontrolled factors and time trends. Such parameters as temperature (ambient) and pH (6.8–7) were kept constant.

Data analyses, determination of empirical models and response surfaces, as well as optimization were carried out using STATISTICA7 software (USA). Statistical validation was determined by ANOVA test at 95% confidence level. The experimental values acquired allowed the generation of a matrix with response variables obtained for all reaction conditions (experimental values). Assuming the polynomial non-linear model and applying the Box–Behnken design, the polynomial expressions were calculated for each case. The influence of independent variables and their combination was related to the value and sign of the coefficients of the polynomial expressions.

3. Results and discussion

3.1. Ultrasonic power measurement

The actual power dissipated (P_{diss}) in the reaction mixture is not the same as the ultrasonic output power quoted by the manufacturer (P_m), due to the losses in the ultrasonic energy during the transfer processes. One of the most common methods of measuring P_{diss} is based on calorimetric measurements and assumes that all the power entering the reaction mixture is dissipated as heat [13]. To avoid the heat loss due to the heat radiation from the system, the ultrasonic tank was completely insulated during the power measurement throughout experiments. The P_{diss} is given by Eq. (13):

$$P_{diss} = \frac{dT}{dt \sum m_i C_{pi}} \quad (13)$$

where m_i and C_{pi} are the mass and heat capacity of the materials present in the tank respectively, and dT/dt is the rate of temperature change, calculated as the initial slope of the graph of temperature plotted against the time of exposure to ultrasound as shown in Fig. 1. The dT/dt value was obtained for the initial 60 min of the process time. The power actually dissipated to the system was calculated to be 298 W, whereas the maximum available ultrasonic output power quoted by the manufacturer, was 400 W.

3.2. Catalyst study

3.2.1. XRD study of the catalyst

XRD analysis revealed that the catalyst was amorphous on the nanometer scale, consisting of a coral-like agglomeration of few

Table 1
Factorial design of experiments: experimental and calculated values of coded variables.

Catalyst x_1	Hydrogen peroxide x_2	TOC conversion after 120 min (%) Y_1		TOC conversion after 240 min (%) Y_2		Time of peroxide decomposition (min) T	
		Experimental	Calculated	Experimental	Calculated	Experimental	Calculated
−1	−1	6.0	4.7	9.2	8.5	70.0	97.3
−1	0	11.3	13.4	20.0	20.0	120.0	120.0
−1	1	5.4	4.7	16.3	17.0	220.0	192.7
0	−1	24.0	24.8	31.4	31.4	110.0	55.3
0	0	36.1	35.6	52.2	52.2	48.0	51.3
0	1	29.3	28.9	42.0	42.0	85.0	139.7
1	−1	23.4	23.9	36.2	36.9	52.0	79.3
1	0	38.3	36.7	53.1	53.1	57.0	57.0
1	1	31.0	32.1	46.2	45.5	180.0	152.7

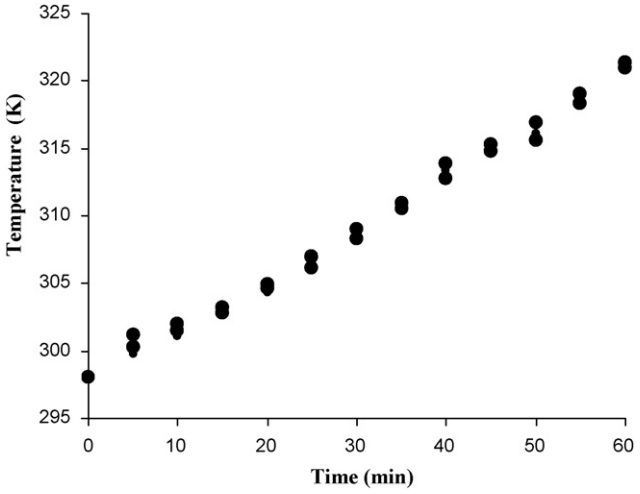

Fig. 1. Determination of ultrasonic power dissipated in the system from the temperature raised in the reaction system.

nanometer-sized clusters, as seen in the high resolution scanning electron micrograph (Fig. 2). Amorphous catalysts lack long-range crystalline order and have unique electronic, catalytic properties and stronger poisoning resistance [1]. No noticeable change in the structure of the samples was detected even after 6 h of ultrasound irradiation treatment, though the catalyst turned to have a bit more amorphous structure than initially observed.

3.2.2. Textural properties of the catalyst

Evolution of textural properties of the catalyst after silent and ultrasound-assisted treatment has been studied by obtaining the N_2 adsorption/desorption isotherms of the catalyst after different times of the reaction. The results are given in Table 2. Fig. 2 depicts particle size distribution of fresh and used catalyst after silent (Fig. 2a and b) and ultrasound-assisted (Fig. 2c) treatment. Average particle size distribution of fresh catalyst was 1032 nm with 90% of particles less than 1655 nm versus 186 nm and 90% distribution less than 277 nm after 6 h of sonication. According to the results presented in Table 2, the particle size is decreasing consistently as a function of sonication time and as a result of fragmentation phenomena breaking catalysts into smaller particles. This was also observed by Kim et al. [7], who determined the proportional correlation between the particle size and sonication time. In fact, BET surface area of the catalyst with the average particle size of 1655 and 277 nm, was 22.59 and 110 $m^2\,g^{-1}$, respectively with no significant changes in the pore size. However, porous structure has been developed greatly after ultrasonic treatment as a result of inter-particle collision [3]. Data in Table 2 indicate that the catalyst essentially became microporous and the contribution of microporosity represented nearly 50% of a fresh catalyst BET surface area. This implies that the ultrasound plays a prominent

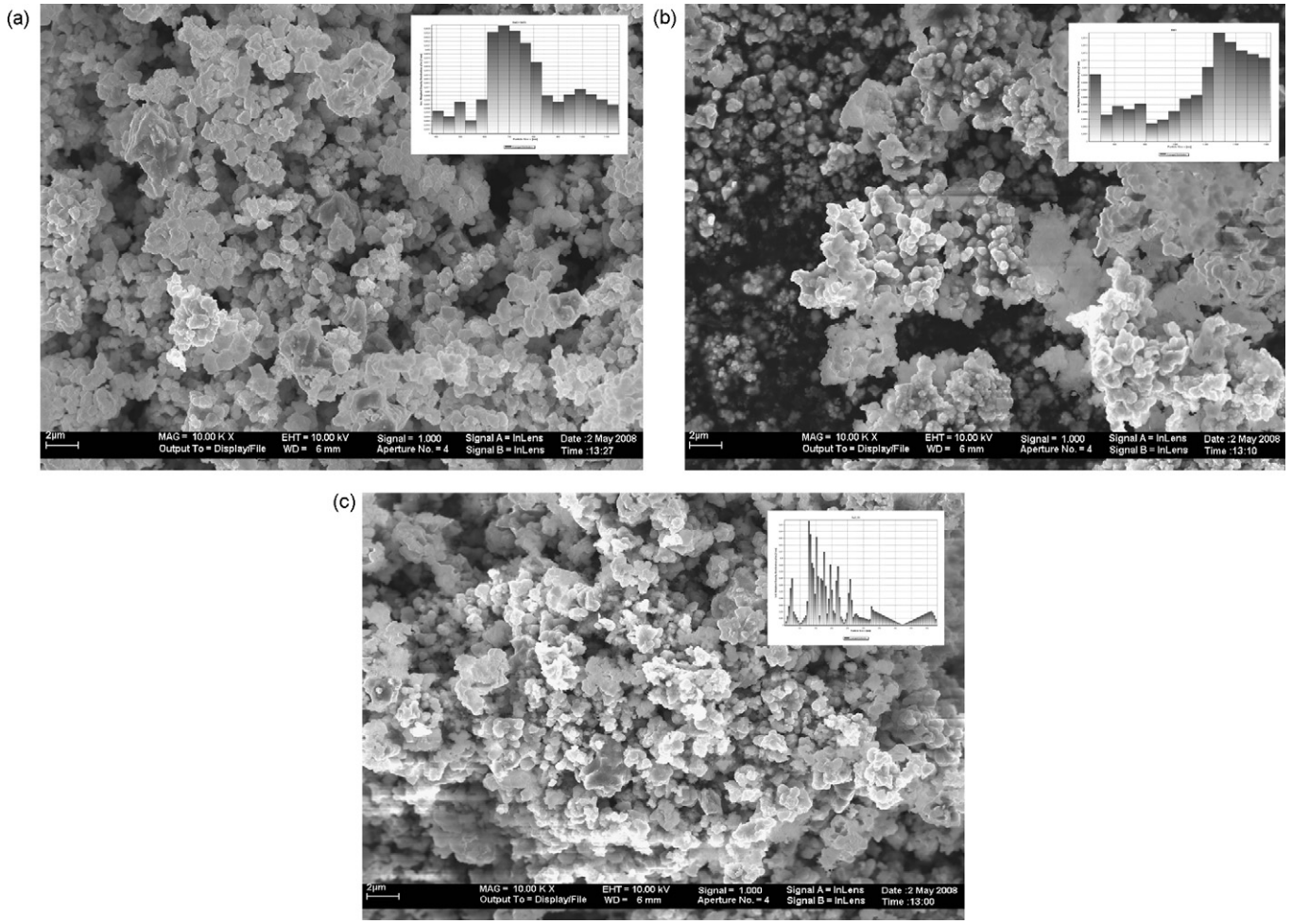

Fig. 2. Representative SEM micrographs of RuI_3 catalysts (a) fresh (b) after silent oxidation and, (c) ultrasound-assisted process (time 6 h, Ph:H_2O_2 = 1:500, 1 g L^{-1} of catalyst). Particle size distributions of catalyst are given as insets.

Table 2
Textural properties of catalyst.

Textural properties of catalyst	Fresh catalyst	After silent treatment		After ultrasound-assisted treatment	
		1 h	6 h	1 h	6 h
Particle size distribution, nm	771–1655	770–1670	1640–2000	582–1099	125–277
BET surface area, $m^2\ g^{-1}$	22.5	18.7	13.5	34.7	110.4
t-Method Micro Pore Surface Area, $m^2\ g^{-1}$	0	0	0	3.56	8.25
BJH Method Cumulative Adsorption Pore Volume, $cm^3\ g^{-1}$	0.1622	0.1524	0.1012	0.1742	0.7590
DR Method Micro Pore Volume, $m^2\ g^{-1}$	0	0	0	0.137	0.414
BJH Method Adsorption Pore Diameter (Mode), Å	13.7	13.7	13.6	13.7	13.6

role in making the material porous as it was also observed by Kim et al. [7].

It can be seen from Table 2 that not only ultrasound-assisted but also the silent oxidation process modifies the textural properties of the catalyst by mainly reducing the BET surface area and the cumulative pore volume. The significant decrease in the surface area (almost 40% after 6 h of the experiment) does not correspond to high phenol conversion but to the susceptibility towards coupling reactions on the catalyst surface, quantified by the decrease in the oxidation rate [3,12]. This was further confirmed by images of the catalyst surface by an electron-scanning microscope before and after exposure to H_2O_2 and ultrasound. Typical SEM micrographs are presented in Fig. 2. The catalyst surface after silent treatment was covered with deposits (Fig. 2b). This could be explained by (I) the formation of reaction by-products, such as tar, formed as a result of further oxidation of primary intermediates dihydroxybenzenes; and (II) oxidation of the catalyst surface itself producing new oxygen containing (surface coordinated H_2O or OH^-) groups [19]. Catalyst surface after silent treatment consisted mainly of slightly aggregated RuI_3 particles with a rate constant $k_s = 0.01197\ s^{-1}$ for 8 h process, resulting in an average particle size up to 2000 nm. Thus, agglomeration of the catalyst was found to be rather limited.

3.2.3. Reactivity of the catalyst

The porous structure has been reported as undesirable for partial oxidation due to diffusive processes that might slow down the reaction [9]. However, calculated turn over frequencies (TOF) of catalysts were 113 and 195 h^{-1} for silent and ultrasound-assisted systems, respectively. This significant difference in TOF was accompanied by a remarkable decrease in the reaction time for sonochemical degradation of phenol, which was particularly evident for 3 h experiments, resulting in 52% phenol removal, whereas the same removal rate was achieved after nearly 6 h of a silent treatment. Thus, improved catalytic behaviour of ultrasound-assisted system is consistent with an improvement in textural structure of RuI_3-increased surface area and microporous structure as a result of inter-particle collision which consequently improved the reactivity of the catalyst [3,19]. These results clearly show that diffusion does not retard oxidation of phenol in the presence of ultrasound but may even enhance the whole process. The probable reason is that the microjets formed during asymmetric cavitation facilitate the liquid to move with a velocity of up to 104 cm s^{-1} resulting in an increased diffusion of solute inside the pores of the specimen [3]. Thus, H_2O_2 reaches the pores itself and higher quantity of $^{\bullet}OH$ is formed as a result of reaction between H_2O_2 and the pore walls of the catalyst.

Mechanical effects of ultrasound, such as turbulence, also enhance the mass transfer on the liquid–solid interface of the reaction system [1]. Spreading of small particles, intensified with turbulence is much faster and tends to improve the accessibility of contaminant to the catalyst surface and thus increasing the collision probability between phenol and active radical species, produced by decomposition of the oxidant on the catalyst active sites. This can be observed by an increase in reactivity of RuI_3 for ultrasound-assisted in comparison to the silent process. Fig. 3 demonstrates a substantial increase in the TOC removal rate (which corresponds to the improved phenol removal rate) and consequently the increase in the reactivity of the catalytic system for sonochemical oxidation in comparison to the silent oxidation applied with identical operational parameters.

3.3. Catalytic oxidation of phenol

The degradation of phenol without initial pH adjustment at constant temperature led to the dominant influence of limited amount of parameters such as catalyst and oxidant concentrations over the process efficiency. However, secondary parameter, such as rotation speed of a reaction mixture stirring was also found to be important. It has been reported that rotation speed is a significant parameter for minimization of external mass-transfer resistance for the species to transfer to the surface of the catalyst and thus, all external mass transfer limitations can be removed by proper mixing [18]. At a lower speed, conversion of phenol was weaker and in the absence of stirring, only 5–7% degradation occurred after 6 h of treatment. Rotational velocities in excess of 800 rpm ensured very good mass transfer between the catalyst and the liquid, due to an internal circulation generated in the reactor. Klaewkla et al. [19] reported that the resistance to mass transfer from the liquid phase to the solid surface is absent at 800–1000 rpm. Beyond the stirring rate of 1000 rpm, a vortex flow pattern occurs and impairs the overall process [20].

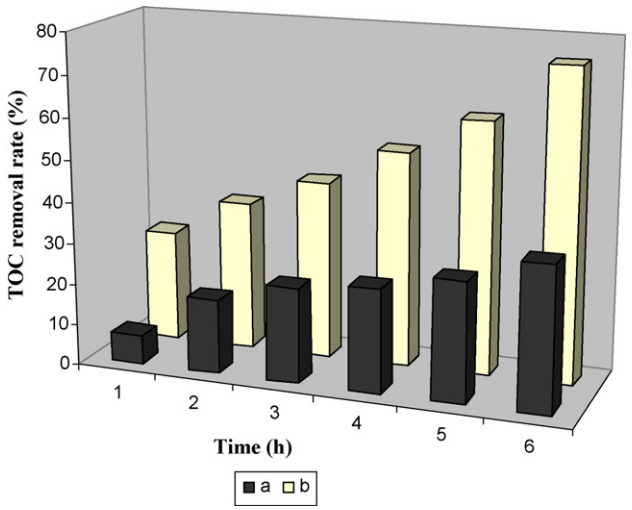

Fig. 3. TOC removal rate after (a) silent (b) ultrasound-assisted treatment (Ph:H_2O_2 = 1:500, 1 g L^{-1} of catalyst, pH 6.8, ambient temperature).

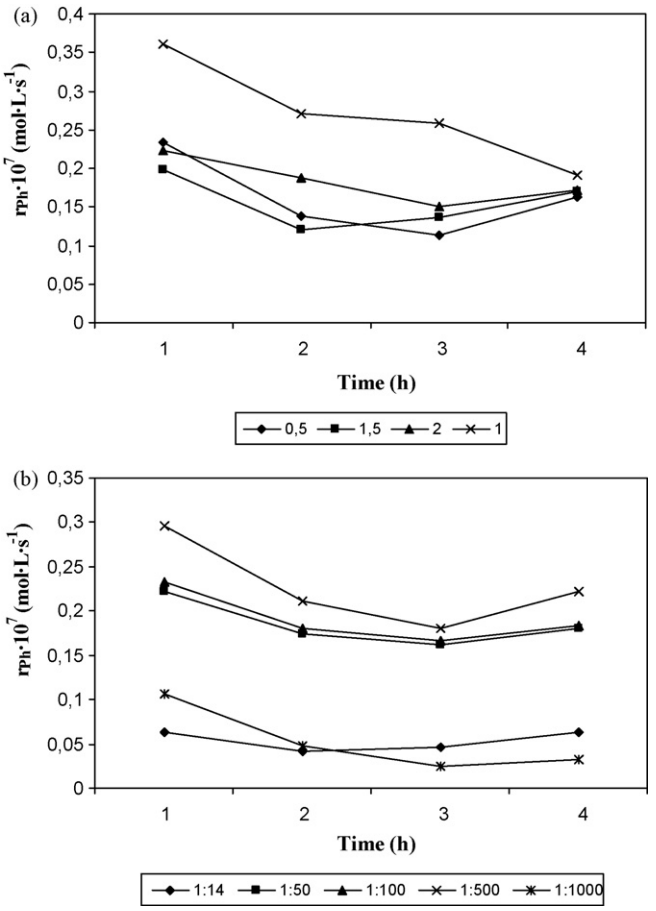

Fig. 4. Phenol degradation rates with different (a) concentrations of the catalyst; (b) molar ratios of phenol:H_2O_2.

The proper selection of reactant concentrations is the crucial point of stoichometric processes. The influence of catalyst loading is depicted in Fig. 4a. It is clearly seen that the highest reaction activity has been observed for the catalyst concentration of 1 g L^{-1}. It is generally accepted that initially phenol oxidation increases with catalyst concentration, then the rate per weight of catalyst levels off and becomes constant [21]. While the surface area of the catalyst plays an ambiguous role, the amount of catalyst is also very important. As the oxidation process takes place in the bulk solution, catalytic activity decreases with an increase in the catalyst mass [14]. This may explain why the degradation rate of phenol increased with an increase in the weight of catalyst up to an optimum loading of 1 g L^{-1}. Moreover, it is determined for reactions with ultrasound that thermal decomposition at the interfacial region is predominant at relatively high substrate concentrations (as in the current study), while at low concentrations free radical reactions are likely to prevail [22].

Theoretically, 14 mol of hydrogen peroxide are needed to completely degrade 1 mol of phenol. However, in practice, excess amounts of hydrogen peroxide are actually used to obtain efficient phenol degradation. Correlation between the amount of hydrogen peroxide and phenol is not directly proportional, and at some concentration levels, hydrogen peroxide may act as a radical scavenger, or the residual hydrogen peroxide may also contribute to additional contamination (e.g. increase in chemical oxygen demand (COD)) in the final solution [23]. The effect of hydrogen peroxide concentration is shown in Fig. 4b. The optimum ratio phenol:hydrogen peroxide for the current study was found to be 1:500, being consistent with the literature reports [20]. The effect of 1:1000 ratio has been found to be detrimental to the degradation process in general with a remarkable decrease in the removal rate, producing hydroperoxyl radical as suggested by the following reactions:

$$H_2O_2 + {}^{\bullet}OH \rightarrow H_2O + {}^{\bullet}HO_2 \quad (14)$$

$$H_2O_2 + {}^{\bullet}HO_2 \rightarrow H_2O + {}^{\bullet}OH + O_2 \quad (15)$$

$${}^{\bullet}HO_2 + {}^{\bullet}HO_2 \rightarrow H_2O_2 + O_2 \quad (16)$$

Despite hydroperoxyl radical is a relatively strong oxidant, active towards target compounds, its reactivity is lower compared to the hydroxyl radicals [23].

3.4. Formation of the reactive species and the reaction scheme

Fig. 5 shows the phenol conversion during 6 h of experiments performed during silent and ultrasound-assisted treatment, with various systems: ultrasound alone, ultrasound and hydrogen peroxide, ultrasound with catalyst, catalyst and hydrogen peroxide, and ultrasound with catalyst and hydrogen peroxide, investigated. For given conditions, all the systems showed adequate phenol conversion, especially the catalytically enhanced ones. The lowest conversion of phenol was observed with US alone (1%), whereas the highest (70%) was achieved for ultrasound-assisted system in the presence of both, the catalyst and the oxidant (Fig. 5). It is well documented that hydrogen peroxide may be generated through the recombination of hydroxyl radicals at the gas–liquid interface and/or in the solution bulk [19,22]. The saturation of solution with air or oxygen, provokes peroxyl ($^{\bullet}HO_2$) and more hydroxyl radicals to be formed in the bubble and the recombination of the former at the interface and/or in the solution bulk that results in the formation of additional hydrogen peroxide. Relatively small amount of hydrogen peroxide (10 ppm) has been detected after ultrasound irradiation of deionized water under the same experimental conditions (whereas at least 100 ppm of oxidant is needed to initiate the oxidation reaction). This is in a good agreement with Kim and co-workers [20], who confirmed poor performance of ultrasound alone and justified the use of additional oxidant and catalyst in order to enhance the degradation efficiency. Also, for non-catalytic ultrasound-assisted processes, formed radicals recombine inside the cavitation bubble at high temperature, whereby reducing the overall yield of H_2O_2 [3].

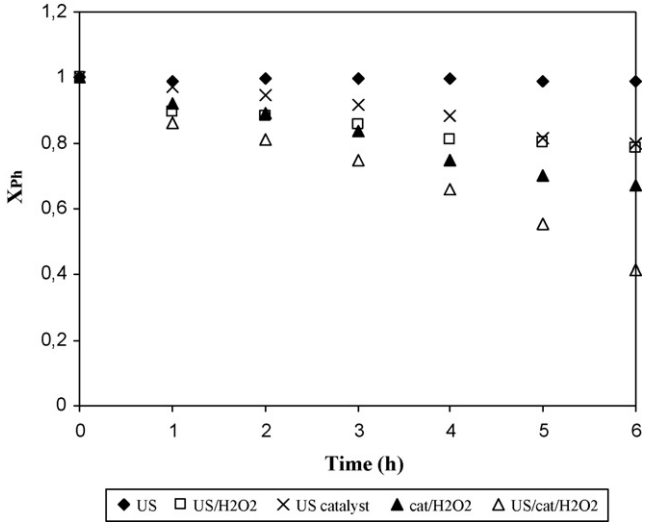

Fig. 5. Conversion of phenol using ultrasound-assisted, hydrogen peroxide and heterogeneous catalytic systems in various combinations (Ph:H_2O_2 = 1:500, 1 g L^{-1} of catalyst).

Catalytic systems showed greater applicability to degrade phenol over non-catalytic systems (Fig. 5). The catalyst/H_2O_2 system was found to be feasible for reactive species production, resulting in 27% of phenol and 35% of TOC conversion after 6 h of experiment. However, time needed for 45% decomposition of phenol and 52% of TOC, significantly decreased for ultrasound-assisted system and was 4 h versus 8 h for the silent catalytic oxidation. It has been found that when ultrasound irradiation is applied, such hydrophilic and semi-volatile compounds as phenol mainly degrade on the interface of cavitation bubble or in the bulk solution via free radical reaction rather than inside of the bubbles via pyrolysis reaction [2]. Ultrasound alone failed to decompose phenol via direct pyrolysis at 24 kHz. The main reason for this may be too low frequency of applied ultrasound that was unable to produce enough radicals and hydrogen peroxide to substantially decompose phenol. Moreover, Petrier et al. [24] who studied different frequencies of ultrasound for phenol degradation reported that the sonochemical phenol degradation proceeds more rapidly at high rather than low frequencies and this can be related to a better release of $^{\bullet}OH$ in the solution in the former case.

During the ultrasound-assisted treatment, the relative importance of hydroxyl radical and thermal decomposition reactions depend on several factors such as the physicochemical properties of the reaction system (i.e. volatility, hydrophobicity, initial concentration, and pH of the liquid phase) and the operating conditions employed (ultrasound frequency, power, presence of saturating gases and/or co-solutes, reactor configuration and geometry) [1]. The horn type sonotrode is only feasible for indirect oxidation of phenol by attacking molecules with formed hydroxyl radicals in the bulk solution or interface between the collapsing bubbles [22]. The reaction mechanism for generation of hydroxyl radicals on Ru^{3+} surface is proposed on the basis of the fundamental reactions describing the surface complexation chemistry for iron and generally accepted Haber Weiss mechanism for the interaction of H_2O_2 with the surface sites and other reactive species:

$$\equiv Ru^{3+} + H_2O_2 \rightarrow \equiv Ru(OOH)^{2+} + H^+ \leftrightarrow \equiv Ru^{2+} + {}^{\bullet}HO_2 + H^+ \quad (17)$$

$$\equiv Ru(OOH)^{2+} \xrightarrow{)))} \equiv Ru^{2+} + {}^{\bullet}HO_2 \quad (18)$$

$$\equiv Ru^{2+} + H_2O_2 \rightarrow \equiv Ru^{3+} + OH^- + {}^{\bullet}OH \quad (19)$$

$$\equiv Ru^{3+} + {}^{\bullet}HO_2 \rightarrow \equiv Ru^{2+} + H^+ + O_2 \quad (20)$$

$$2{}^{\bullet}HO_2 \rightarrow H_2O_2 + O_2 \quad (21)$$

$$O_2 + {}^{\bullet}H \rightarrow {}^{\bullet}HO_2 \quad (22)$$

$$H_2O_2 \xrightarrow{)))} 2{}^{\bullet}OH \quad (23)$$

The driving force of the process is free radicals, formed as a result of hydrogen peroxide decomposition over solid catalyst (reactions (17) and (19)), recombination of radicals (reactions (14)–(16), (21) and (22)) and ultrasonically enhanced decomposition (reaction (23)). In the presence of ultrasound, additional free hydroxyl radicals can also be formed (reactions (1), (18), (23)). Not all the generated $^{\bullet}OH$ radicals can induce phenol degradation, because with such an elevated concentration of $^{\bullet}OH$ at the air–water interface, radical–radical recombination to yield H_2O_2 and H_2O would be much more pronounced than the reaction with the substrates, and therefore would also limit the diffusion of reactive radical species to the solution bulk [2]. The simplified scheme of the process can be introduced as a sequence of reactions of interaction between active sites of the catalyst, free radicals, hydrogen peroxide and their recombination, taking place on the catalyst surface, in the bulk solution or interface between the cavitation bubbles. The limiting step of the reaction, according to the proposed scheme is the reduction of Ru^{3+} to Ru^{2+} mediated by the formation of $Ru(OOH)^{2+}$ complex [3]. Reaction (18) shows the improved dissociation of the complex in the presence of ultrasound, enhancing the amount of catalytic active sites, as it is discussed earlier. Moreover, Ru^{3+} active sites of the catalyst can react with hydroperoxy radicals according to the reaction (20) to produce more Ru^{2+} sites, which subsequently increase the reaction rate (19).

In order to confirm free radical mechanism and the importance of hydroxyl radicals for the degradation of phenol, radical scavenger have been added to the reaction mixture. The reaction significantly slowed down (in average by 40%), however was still 15% higher in comparison to a silent mode. Consequently, the presence of other than $^{\bullet}OH$ reactive species is also assumed. It is argued that upon ultrasonic irradiation, iodide can be liberated from solutions such as potassium iodide saturated with air [2]. Also, Minero et al. [25] reported that during sonication in the presence of iodides, radical species $^{\bullet}I_2^-$ may be formed, which may also act as weak oxidising agents. Despite iodides have been known as radical scavengers, quenching of $^{\bullet}OH$ by the iodine anions may yield additional radical species, reactive towards the organic compounds, such as phenol, according to reactions:

$$^{\bullet}OH + I^- \rightarrow OH^- + {}^{\bullet}I \quad (24)$$

$$^{\bullet}I + I^- \rightarrow {}^{\bullet}I_2^- \quad (25)$$

The beneficial role of new reactive species adds to the hypothesis that $^{\bullet}I_2^-$ undergo more limited radical–radical recombination compared to $^{\bullet}OH$ on the surface of the cavitation bubbles [26]. In such a way new radicals can be more available than $^{\bullet}OH$ to attack phenol molecules instead and induce their decomposition. Accordingly, anions may transform $^{\bullet}OH$ into less reactive species that can, however, be involved at a higher extent in a substrate transformation. Considering that, if not reacting with the anions, $^{\bullet}OH$ would mainly undergo recombination, and degradation enhancement would only be possible if the reaction rate between the added anions and $^{\bullet}OH$ was higher than that between phenol and $^{\bullet}OH$, although both would be much lower than the rate of radical–radical recombination (reactions (14) and (19)) [27].

3.5. Factorial design of the ultrasound-assisted oxidation system

Experimental factorial design study (3^2) was accomplished at three levels of −1, 0 and +1 and the results are shown in Table 1 for both, the predicted and calculated values. The main effects and two factor interactions based on the responses were used to describe factor contribution to the removal efficiency. The following equations are the ultimate model resulting from ANOVA analysis in terms of coded factors for TOC removal efficiency:

$$Y_1 = 35.6(\pm0.66) + 11.6(\pm1.09)x_1 - 10.6(\pm1.89)x_1^2 + 2.1(\pm1.09)x_2 - 8.72(\pm1.89)x_2^2 + 4.1(\pm1.97)x_1x_2 \quad (26)$$

$$Y_2 = 52.2(\pm0.48) - 16.6(\pm1.18)x_1 - 15.7(\pm1.02)x_1^2 + 5.3(\pm1.18)x_2 - 15.5(\pm1.02)x_2^2 + 0.7(\pm1.28)x_1x_2 + 20.5(\pm1.29)x_1x_2^2 \quad (27)$$

$$T = 51.3(\pm1.42) + 20.2(\pm0.89)x_1 - 35.5(\pm0.89)x_1^2 + 42.2(\pm2.11)x_2 - 44.5(\pm1.29)x_2^2 \quad (28)$$

Multivariate non-linear regression correlation coefficients, R^2, for Eqs. (26)–(28) were 0.985, 0.997 and 0.998, respectively. Model parameters, estimated from experimental values are shown in Table 1. Corresponding model coefficients and confidence intervals (within brackets) are presented in Eqs. (26)–(28).

Represented equations fit the experimental data obtained, and Fig. 6 shows the relationship between the experimental and the predicted values. It may be clearly seen that values calculated with the predictive equations are very close to the experimentally observed ones.

Considering influence of independent variables with the coefficients of Eqs. (26)–(28), it is obvious that dependence of each equation is non-linear according to the selected model and thus is represented by the curved surfaces. Graphically depicted response surfaces are shown in Fig. 7. No antagonistic effects between the variables were observed. Quadratic effects of two variables indicate that maximum values can be found for each parameter. The both variables (catalyst and hydrogen peroxide concentrations) were found important, however, a negative effect was observed in both cases, such as an excess of catalyst (x_1^2) and hydrogen peroxide (x_2^2) (Eqs. (26)–(28)). This observation was confirmed by Fig. 7, where the reactivity of the catalyst was decreasing with increased concentrations of reactants. 3D response surface at 120 min (Fig. 7a) showed an improved conversion of TOC with an increase in catalyst loadings.

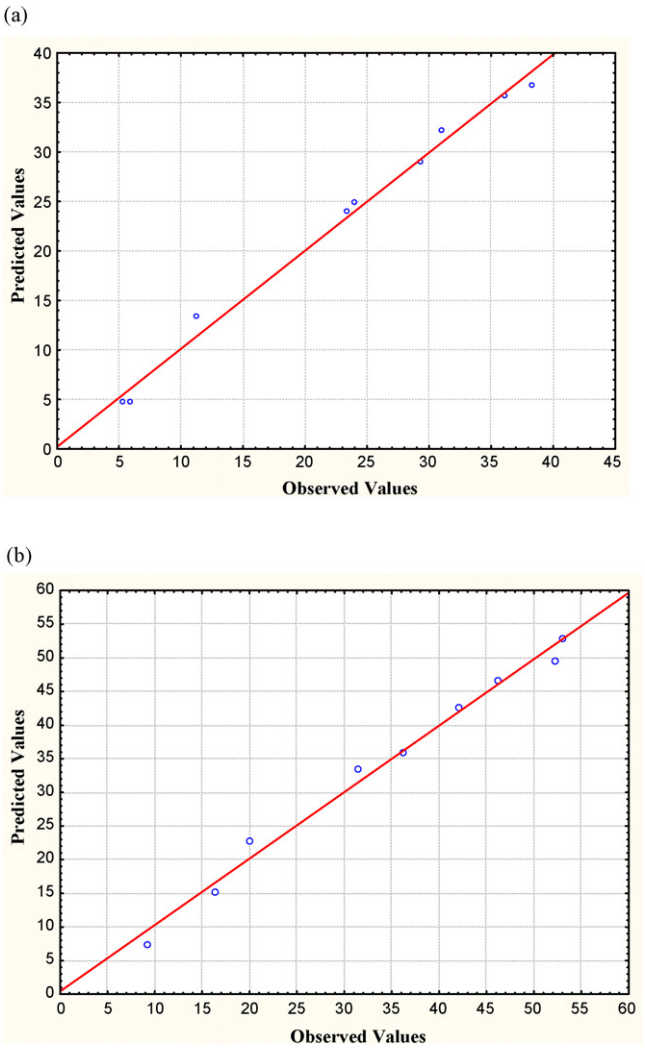

Fig. 6. Accuracy of predicted data with respect to the experimental values for Y_1 and Y_2.

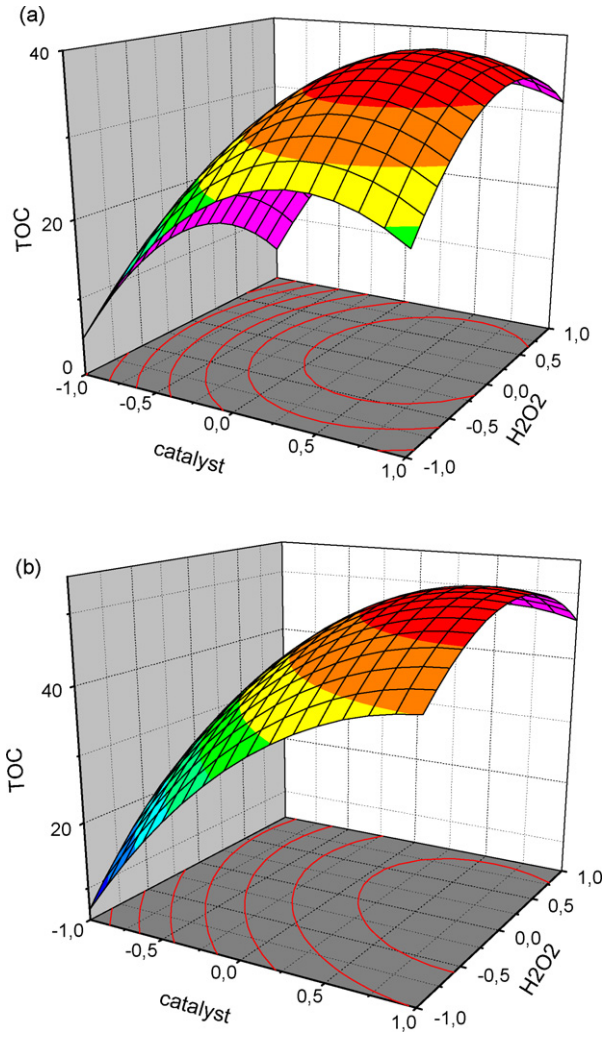

Fig. 7. 3D response surfaces and contour plots of TOC conversion efficiency showing the interacting effect of [H_2O_2] and [catalyst] after (a) 120 min (Y_1), (b) 240 min (Y_2) of experiment.

This trend was observed for all oxidant concentrations range studied at 240 min as well (Fig. 7b). This observation was reflected by the relatively high value of x_1 and low value of the x_2 linear coefficients and the statistically significant values of quadratic coefficients in Eqs. (26) and (27). The influence of catalyst loading on TOC removal, was more significant than the influence of oxidant concentration, however the tendency of TOC removal dropped with an increase in the catalyst loading. The extent of TOC degradation was less sensitive to x_2 within the medium (0) to high (+1) concentration range. For TOC degradation at 240 min, the influence of reactants concentrations demonstrated a synergetic effect ($x_1x_2^2$) as it was pointed out in Eq. (27). The TOC removal rate consistently reached its maximum for both time intervals for medium to high catalyst loading and medium hydrogen peroxide level. High positive regression coefficients indicated that there was a strong correlation between independent variables and obtained results.

It is generally accepted for such organic substances, that an increase in the H_2O_2 concentration produces an increase in both, the initial mineralization rate and the final degradation of the organic material [5]. The time necessary to achieve complete hydrogen peroxide decomposition (T) has been studied and results are presented in the contour plot (Fig. 8). It shows that time is dependable on the concentrations of hydrogen peroxide and the catalyst. Large positive values featured by x_1 and x_2 regression

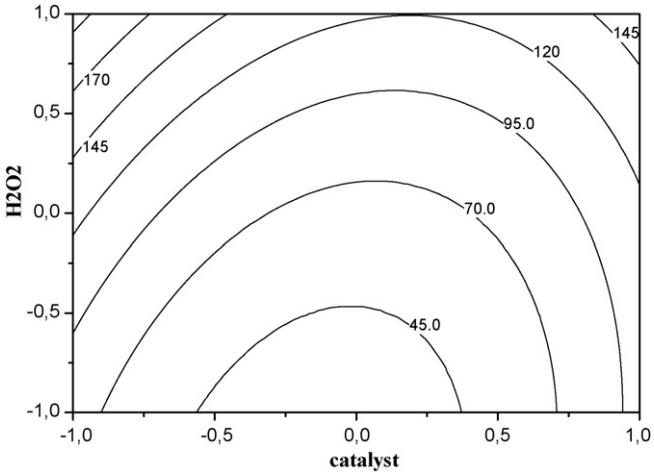

Fig. 8. Contour plot of time required to achieve total consumption of H_2O_2 by ultrasound-assisted oxidation, as a function of initial RuI_3 and H_2O_2 concentrations.

coefficients in Eq. (28), indicated that time of consumption increased with an increase in H_2O_2 doses; moreover, T increased when initial catalyst concentration also increased. Especially at high RuI_3 concentrations T tended to increase, as described by the large negative x_2 quadratic coefficient (-44.5) in Eq. (28). Thus, hydrogen peroxide consumption positively correlated with the oxidant and catalyst concentrations throughout the course of experiments. It is well documented that extreme catalyst and oxidant concentrations reduce the efficiency of organic pollutant removal [3,6,22]. Indeed, the excess of reactants could act as $^{\bullet}OH$ radical scavengers (reactions (14)–(16)). Accordingly, the increase in H_2O_2 feeding showed detrimental effect due to the scavenging effect and did not promote any TOC conversion. Moreover, the total consumption of hydrogen peroxide was reached within 1 h at medium level of variables (Fig. 8).

3.6. Reusability and stability of the catalyst

Reusability of RuI_3 for the degradation of phenols by silent and ultrasound-assisted oxidation with H_2O_2 was estimated. The solution resulting from the degradation of phenols was filtered, washed gently with deionized water (>17.7 MΩ) and the catalyst was dried in air without any additional treatment. The dried catalyst samples were used for oxidation of phenols, employing similar conditions as in previous experiments. It was observed that dissolution of RuI_3 was found to be negligible (0.002% loss of ruthenium was observed during 8 h of reaction time without and 0.005% with ultrasonic irradiation). The percentage reduction in the rates of silent (6%, 5%, and 6%) and ultrasound-assisted (6%, 10% and 8.5%) oxidation over RuI_3 after three cycles was found, respectively, for every subsequent cycle. RuI_3 samples showed considerably reproducible catalytic activity up to three cycles for the degradation of phenols regardless the catalyst concentration. The loss in ruthenium catalyst activity was more pronounced only after fourth cycle of the reuse.

4. Conclusion

Developed system (RuI_3/H_2O_2/US) revealed to be feasible to efficiently degrade phenol in aqueous solution. Selected catalyst benefited circum neutral pH and ambient temperature at atmospheric pressure as operation window. RuI_3 exhibited outstanding stability and high reusability at chosen process conditions. The parameters, strongly affecting the reaction, were major parameters of the process such as reactants concentrations and hydrogen peroxide feed. The free radical mechanism was assumed for ultrasound-assisted oxidation process, which was validated qualitatively by means of strong radical scavengers. Fractional factorial design showed that medium values of the catalyst and H_2O_2 concentrations were optimal to achieve the highest (up to 55%) TOC degradation within 4 h of the experiment. The contour plot of time, needed for complete hydrogen peroxide decomposition showed that the best interval lies within 1 h.

Ultrasound irradiation played a prominent role in the modification of catalyst textural properties, producing microporous structure with higher surface area as a result of fragmentation of the catalyst particles. Moreover, it had a promotional effect, preventing agglomeration of catalyst particles and improving the accessibility of phenol and hydrogen peroxide to the catalyst active sites.

The two-fold increase in ultrasound-assisted process efficiency in comparison to silent oxidation process was attributed to improved catalytic behaviour of the catalyst and generation of oxidizing species such as $^{\bullet}OH$, $^{\bullet}HO_2$ and $^{\bullet}I_2^-$ via hydrogen bonds cleavage and recombination of radicals. However, disadvantage of new oxidative species may be the formation of reaction by-products. Thus, the detailed mechanism of the reaction would merit further investigation with determined full set of intermediates and oxidation products.

Acknowledgements

Ekokem Oy foundation and Academy of Finland (decision number 212649) are acknowledged for their financial support of the research. Authors also wish to thank Ms. E. Reppo for ICP–OES measurements.

References

[1] K.S. Suslick, Applications of ultrasound to heterogeneous catalysis, in: Advances in Catalyst Preparation, Catalytica Studies Division, Mountain View California, 1995
[2] R.S. Disselkamp, K.M. Judd, T.R. Hart, C.H.F. Peden, G.J. Posakony, L.J. Bond, J. Catal. 221 (2004) 347–353.
[3] S. Parsons, Advanced Oxidation Processes, IWA Publishing, Netherlands, 2004p. 356.
[4] D. Drijvers, H. van Langenhove, M. Beckers, Water Res. 33 (1999) 1187–1194.
[5] R. Molina, F. Martinez, J.A. Melero, D.H. Bremner, A.G. Chakinala, Appl. Catal. B: Environ. 66 (2006) 198–207.
[6] M. Kitis, S.S. Kaplan, Chemosphere 68 (2007) 1846–1853.
[7] J.K. Kim, F. Martinez, I.S. Metcafe, Catal. Today 124 (2007) 224–231.
[8] M.H. Entezari, C. Petrier, Ultrason. Sonochem. 10 (2003) 241–246.
[9] L. Davydov, E.P. Reddy, P. France, P.G. Smirniotis, Appl. Catal. B: Environ. 32 (2001) 95–105.
[10] M. Papadaki, R.J. Emerya, M.A. Abu-Hassan, A. Dıaz-Bustos, I.S. Metcalfe, D. Mantzavinos, Sep. Purif. Technol. 34 (2004) 35–42.
[11] M. Shimizu, H. Orita, T. Hayakawa, Y. Watanabe, K. Takehira, Bull. Chem. Soc. Jpn. 64 (1991) 2583–2584.
[12] S.-S. Lin, M.D. Gurol, Environ. Sci. Technol. 32 (1998) 1417–1423.
[13] L.C. Hagenson, L.K. Doraiswamy, Chem. Eng. Sci. 53 (1998) 131–148.
[14] M. Stoyanova, St. Christoskova, M. Georgieva, Appl. Catal. A: Gen. 249 (2003) 295–302.
[15] X.-S. Chai, Q.X. Hou, Q. Luo, J.Y. Zhu, Anal. Chim. Acta 507 (2004) 281–284.
[16] A. Georgi, F.-D. Kopinke, Appl. Catal. B: Environ. 58 (2005) 9–18.
[17] M. Perez-Moya, M. Graells, L.J. del Valle, E. Centelles, H.D. Mansilla, Catal. Today 124 (2007) 163–171.
[18] A. Quintanilla, N. Menendez, J. Tornero, J.A. Casas, J.J. Rodrıguez, Appl. Catal. B: Environ. 81 (2008) 105–114.
[19] R. Klaewkla, S. Kulprathipanja, P. Rangsunvigit, T. Rirksomboon, W. Rathbun, L. Nemeth, Chem. Eng. J. 129 (2007) 21–30.
[20] J.K. Kim, I.S. Metcalfe, Chemosphere 69 (2007) 689–696.
[21] J. Guo, M. Al-Dahhan, Ind. Eng. Chem. Res. 42 (2003) 2450–2460.
[22] R.M. Liou, S.H. Chen, M.Y. Hung, C.S. Hsu, J.Y. Lai, Chemosphere 59 (2005) 117–125.
[23] K. Maduna Valkaj, A. Katovic, S. Zrncevic, J. Hazard. Mater. 144 (2007) 663–667.
[24] C. Petrier, M.F. Lamy, A. Francony, A. Benahcene, B. David, J. Phys. Chem. 98 (1994) 10514–10520.
[25] C. Minero, P. Pellizzari, V. Maurino, E. Pelizzetti, D. Vione, Appl. Catal. B: Environ. 77 (2008) 308–316.
[26] K. Okitsu, K. Iwasaki, Y. Yobiko, H. Bandow, R. Nishimura, Y. Maeda, Ultrason. Sonochem. 12 (2005) 255–262.
[27] M.H. Perez, G. Penuela, M.I. Maldonado, O. Malato, P. Fernandez-Ibanez, I. Oller, W. Gernjak, S. Malato, Appl. Catal. B: Environ. 64 (2006) 272–291.